Analyst

PAPER

View Article Online
View Journal | View Issue

Cite this: *Analyst*, 2016, **141**, 1966

A portable SERS method for the determination of uric acid using a paper-based substrate and multivariate curve resolution

Javier E. L. Villa and Ronei J. Poppi*

This paper presents a portable quantitative method for the on-site determination of uric acid in urine using surface-enhanced Raman spectroscopy (SERS) and gold nanoparticle-coated paper as a substrate. A procedure was developed for the rapid preparation of cost-effective SERS substrates that enabled the adequate control of a homogeneous active area and the use of small quantities of gold nanoparticles per substrate. The standard addition method and multivariate curve resolution-alternating least squares (MCR-ALS) were applied to compensate for the matrix effect and to address overlapping bands between uric acid and interference SERS spectra. The proposed methodology demonstrated better performance than conventional univariate methods (in terms of linearity, accuracy and precision), a wide linear range (0–3.5 mmol L^{-1}) and an adequate limit of detection (0.11 mmol L^{-1}). For the first time, a portable SERS method coupled with chemometrics was developed for the routine analysis of uric acid at clinically relevant concentrations with minimal sample preparation and easy extension for the on-site determination of other biomarkers in complex sample matrices.

Received 19th November 2015,
Accepted 26th January 2016

DOI: 10.1039/c5an02398j

www.rsc.org/analyst

1. Introduction

Uric acid is the end product of the catabolization of purine nucleotides and is considered to be an important biomarker in urine and serum.[1] Previous studies have shown that high uric acid concentrations in these biological fluids can be associated with renal diseases[2] and preeclampsia, a hypertensive disorder that occurs during pregnancy and is the primary cause of maternal morbidity and mortality worldwide (more than 50 000 deaths per year), mainly in developing countries.[1,3] Currently, there is no single reliable, cost-effective screening test for preeclampsia and no well-established measures for primary prevention. However, the monitoring, *inter alia*, of uric acid levels in the urine and serum can identify hypertensive pregnant women with a propensity toward superimposed preeclampsia.[4,5]

The most widely employed methods for uric acid determination in urine and serum are limited by the use of expensive enzymes and the time-consuming nature of assay-based tests.[6–9] Methodologies based on liquid chromatography and capillary electrophoresis have also been reported.[10,11] However, the use of organic solvents, the associated laborious sample preparation and extended measurement durations make the analysis unsuitable for rapid and routine uric acid monitoring.

Raman spectroscopy is a powerful technique that has shown progress in applications because it can provide chemical and structural information with minimal sample preparation.[12] Moreover, in recent years, the development of portable Raman spectrometers introduced the possibility of rapid on-site detection in a wide variety of sample types.[13–16] The low efficiency of inelastic scattering restricted the use of Raman spectroscopy to relatively high concentration analyses; nevertheless, surface-enhanced Raman spectroscopy (SERS) is an interesting alternative to overcome this limitation. SERS can dramatically increase the efficiency of Raman scattering through a combination of electromagnetic and chemical contributions when the target molecule (analyte) is attached to the surface of metallic nanostructures (typically made of gold or silver).[17,18] The characteristics of these metallic nanostructures play an important role in their application and particularly quantitative analytical methods for remote and routine analysis require (in the first instance) inexpensive, reproducible and sensitive SERS substrates.[19]

The literature reports several applications of SERS methods for the highly sensitive detection of analytes in aqueous solution even at the single-molecule level.[20–23] However, these methods may not be extended to perform a quantitative analysis in real samples because unpredictable changes from external non-controllable parameters (sample matrix) can occur;

Institute of Chemistry, University of Campinas, P.O. Box 6154, 13081-970 Campinas, SP, Brazil. E-mail: ronei@iqm.unicamp.br

these require an appropriate strategy to address this effect. Additionally, depending on the type of matrix analyzed, overlapping bands can also be an important limitation during the development of quantitative SERS methods due to interferences present in the samples.[24,25] The standard addition method and multivariate curve resolution-alternating least squares (MCR-ALS) have been successfully employed in chromatography to overcome similar problems of the matrix effect and overlapping bands;[26–28] however, their use is rare in quantitative SERS analysis.

Therefore, to be considered an efficient alternative to conventional analytical methods, a SERS-based approach should be rapid, reproducible and capable of performing remote uric acid determination in urine at clinically relevant concentrations ($\geq$0.4 mmol L^{-1}) even in the presence of interferences. To achieve this goal, the primary objectives of this work were (i) to develop a rapid procedure for the preparation of cost-effective SERS substrates, (ii) to apply a standard addition method to compensate for the matrix effect in urine analysis, (iii) to build a calibration curve for uric acid quantification in the presence of interferences using MCR-ALS, and (iv) to validate a MCR-ALS-based method for the determination of uric acid in synthetic urine.

2. Algorithm and data analysis

Multivariate curve resolution is a generic denomination of a family of methods based on the bilinear decomposition of a matrix **D** in scores (**C**) and loadings (**S**) containing information about samples and variables, respectively (eqn (1)).[29]

$$\mathbf{D} = \mathbf{C}\mathbf{S}^{\mathrm{T}} + \mathbf{E} \quad (1)$$

The MCR-ALS algorithm can be summarized in three steps. First, **C** is estimated from **D** and an initial **S**, which is estimated using PURE,[30] SIMPLISMA[31] or from known data (eqn (2)). The **C** matrix is then employed for a new estimation of **S** using eqn (3).[32]

$$\hat{\mathbf{C}} = \mathbf{D}(\mathbf{S}^{\mathrm{T}})^{+} \quad (2)$$

$$\hat{\mathbf{S}}^{\mathrm{T}} = \mathbf{C}^{+}\mathbf{D} \quad (3)$$

Finally, the calculations are repeated several times until the error reaches a minimal value (eqn (4)).

$$\text{Error} = \min \| \mathbf{D} - \mathbf{C}\mathbf{S}^{\mathrm{T}} \| \quad (4)$$

To perform a standard addition analysis *via* MCR-ALS, the spectroscopic data are arranged in a matrix **D** ($r \times c$) with the levels of addition in rows and intensities in columns (Fig. 1). MCR-ALS decomposes matrix **D** using the initial estimate of the spectroscopic profiles (first and last row from matrix **D**). For m species, concentration profiles are described using matrix **C** ($r \times m$); spectral contributions are given in matrix $\mathbf{S}^{\mathrm{T}}$ ($m \times c$), and **E** ($r \times c$) is the matrix of residuals that are not explained.

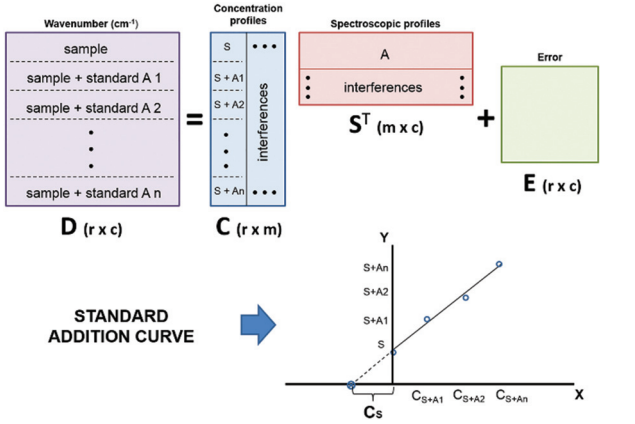

Fig. 1 MCR-ALS arrangement for the standard addition method (*Cs* is the analyte concentration in the sample).

In this work, MCR calculations were performed using MatLab in conjunction with MCR-ALS Toolbox 2.0.[33]

3. Experimental section

3.1 Instrumentation

A Mira M-1 portable Raman spectrometer (Metrohm, Herisau, Switzerland) equipped with a 785 nm source and a maximum laser output power of 75 mW was employed to obtain the spectra. This enabled remote sampling (on-site), high sensitivity and rapid data collection. The average spectral resolution was between 12 and 14 cm^{-1}, and the exposure time was in the range of 1.5–2 s for all measurements. The spectra were recorded in a spectral range of 400 to 1800 cm^{-1}.

UV-visible absorption and field emission-scanning electron microscopy (FE-SEM) investigations were performed using a Varian Cary probe 50 UV-Vis spectrophotometer and a FEI Quanta FEG 250 FE-SEM, respectively.

3.2 Chemicals

All solutions were prepared with deionized water (electrical resistivity of 18.2 MΩ cm) provided in a Milli-Q1 Ultrapure Water Purification System (Millipore, Brussels, Belgium). Chloroauric acid ($HAuCl_4$, 30% mm^{-1}), anhydrous sodium citrate ($Na_3C_6H_5O_7$), bovine albumin, citric acid, creatinine, urea and uric acid were purchased from Sigma-Aldrich (Sao Paulo, SP, Brazil). Sodium chloride, sodium dihydrogen phosphate and potassium chloride were purchased from Merck (Darmstadt, Germany). Laser printer paper with 70 g m^{-2} purchased from Chamex (Sao Paulo, SP, Brazil) was used to prepare all the SERS substrates.

3.3 Preparation of gold nanoparticles and paper-based SERS substrates

In this work, gold nanoparticles (GNPs) were selected instead of silver nanoparticles due to their higher chemical stability and facile synthesis. The synthesis of colloidal GNPs was

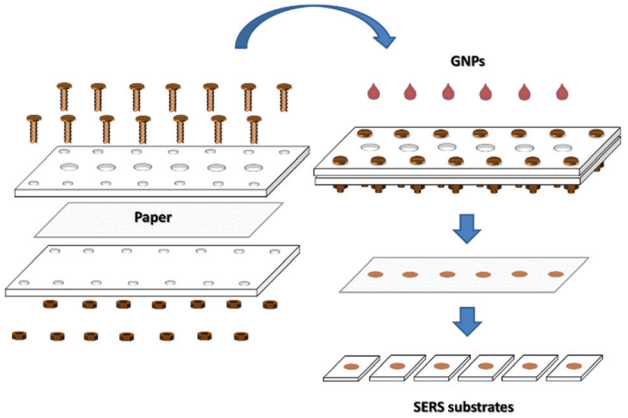

Fig. 2 Proposed procedure for the rapid preparation of paper-based SERS substrates.

based on the Turkevich method because it provides a rapid, simple and reproducible method to obtain homogeneous GNPs.[34] Briefly, an aliquot of 40 μL $HAuCl_4$ solution (30%, mm^{-1}) was pipetted into approximately 100 mL of deionized water and heated under constant stirring. After achieving the boiling point, 1.4 mL of anhydrous sodium citrate solution (2%, mv^{-1}) was added to the mixture under magnetic stirring and, after five minutes, the agitation was interrupted and colloidal GNPs were cooled to room temperature. The GNPs were centrifuged at 3000 rpm for 15 min; 90% of the supernatant was then discarded.

The SERS substrates used in this work were prepared using the proposed system shown in Fig. 2. This system consists of two Teflon templates, one of which has six circular holes (0.4 cm in diameter) used for controlling the active area of the SERS substrates. Printing paper was placed between the two Teflon templates, and aliquots of 20 μL of GNPs were added. The system was then placed in an oven at 80 °C for approximately 80 min. Finally, the SERS substrates obtained were individually cut and coated on pieces of glass measuring 1 × 1 cm^2.

3.4 Quantitative determination of uric acid in synthetic urine

Synthetic urine with and without uric acid was prepared taking into account the majority components (potential SERS interferences) of the real urine matrix of a healthy person.[35,36] Thus, to obtain approximately 1 L of synthetic urine, 10 g of urea, 5.2 g of NaCl, 4.5 g KCl, 4.8 g of NaH_2PO_4, 0.4 g of citric acid, 0.8 g of creatinine and 50 mg of albumin were mixed with 900 mL of deionized water. Then, the pH was adjusted to 6.0 with diluted NaOH or HCl, and the volume was supplemented with deionized water to obtain a specific gravity of approximately 1.1 g cm^{-3}.

Normal Raman spectroscopy was tested for uric acid concentrations at 2, 5 and 10 mM and no Raman spectra were observed, thereby indicating that SERS should be used for uric acid quantification at these concentration levels. To minimize the duration of sample preparation, the analyses were performed *via* simple dilution and, after several tests, a sample dilution of 1% was selected. The uric acid SERS spectra experienced an increasing intensification with the time of incubation tested (from 5 to 30 min). However, after the incubation time of 15 min there was no significant variation in the uric acid SERS spectra. Thus, the SERS substrates were dipped for 15 min and dried prior to analysis. All experiments were carried out in triplicate.

4. Results and discussion

4.1 Characterization of gold nanoparticles and SERS substrate preparation

Colloidal gold nanoparticles (GNPs) were characterized *via* UV-Vis spectroscopy and FE-SEM microscopy; these studies enabled the calculation of the maximum absorption wavelength (534 nm) and the mean particle diameter (47 ± 9 nm, N = 80). The results obtained are in agreement with the expected correlation between the mean particle diameter and maximum absorption wavelength reported by Njoki *et al.*[37] The particle size is adequate for SERS analysis based on studies performed by Hong *et al.* and Bell *et al.* indicating that particle diameters of approximately 46 and 50 nm, respectively, may provide an optimum SERS signal intensification.[38,39]

Previously described procedures for the preparation of SERS substrates based on GNP-coated paper involved dipping a piece of paper into a GNP solution (10 mL per substrate) for a relatively long duration (at least 24 h).[40–42]

To improve this procedure, a simple system (Fig. 2) was employed. The type of paper used and the preconcentration level of colloidal GNPs prior to deposition are two important parameters in obtaining an efficient and reproducible SERS substrate in the proposed procedure. This case considers the higher number of fibers per area compared with filter paper and the possibility of minimizing the amount of GNPs added without the loss of intensity; thus, printing paper and a 10-fold preconcentration level prior to GNP deposition were selected to promote the agglomeration of the GNPs ("hot spots" generation) on the paper surface.[43] The principal advantages of the proposed procedure include better control of the active area, lower numbers of GNPs used per substrate (0.2 mL of GNPs), a reduction in the preparation time (80 min) and easy handling after GNP deposition. The FE-SEM image of GNPs and SERS substrates after GNP deposition shown in Fig. 3 demonstrates that a homogeneous and densely packed GNP deposition over printing paper fibers was achieved to provide a high number of SERS hot spots and to generate a SERS spectra enhancement of molecules near the active surface.

4.2 Considerations regarding the matrix effect and overlapping bands

A study of synthetic urine was performed to develop a quantitative method to quantify uric acid in a complex sample matrix. Fig. 4A shows the SERS spectra obtained for uric acid

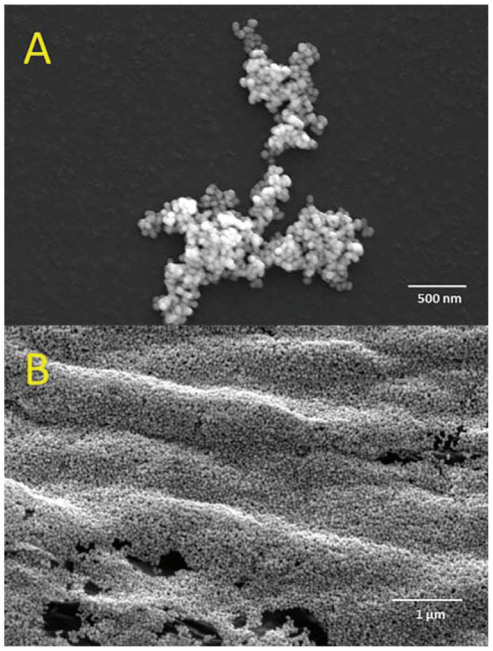

Fig. 3 FE-SEM microscopy of GNPs (A) and GNP-coated paper (B).

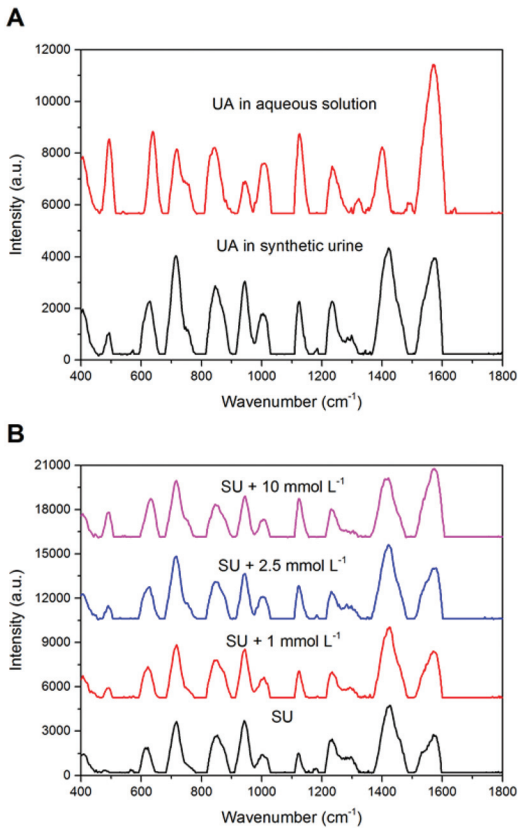

Fig. 4 Matrix effect evaluation for uric acid (UA) in aqueous solution and in synthetic urine (SU) medium (A) and the effect of various uric acid additions to synthetic urine (B).

in aqueous solution and in synthetic urine matrix. The intensity of several bands of uric acid SERS spectra decreases in the presence of a synthetic urine matrix, primarily at 493 cm^{-1} (C–N–C ring vibrations), 633 cm^{-1} (skeletal ring deformation), 1016 cm^{-1} (ring vibration), 1130 cm^{-1} (mixed vibrations) and 1550 cm^{-1} (C–N stretching). This can be explained by the competition between uric acid and non-targeted compounds in the matrix, which can limit the qualitative and quantitative analyses, primarily for a complex sample matrix.[25,44] However, the intensification of the bands at 725 cm^{-1} (N–H bending) and 1398 cm^{-1} (mixed vibration) was observed due to the contribution of compounds present in the synthetic urine matrix on the SERS spectra. These observations demonstrate that an external calibration in aqueous solution is not adequate for quantitative SERS analysis in a synthetic urine matrix; this could apply to the quantification of other analytes in complex sample matrices because the target molecule is not isolated in a real sample. Additionally, Fig. 4B shows that in addition to "signal suppression" due to the matrix effect, overlapping bands between uric acid and interferences can be observed (as expected). These interferences for the SERS spectra of uric acid may arise from the substrate background or chemical compounds with similar chemical functions such as creatinine and urea (which are normally present in the urine at higher concentrations than uric acid). Thus, a sample preparation (*via* dilution) cannot be used to solve this problem.

4.3 MCR-ALS and addition standard method

Synthetic urine was spiked with known concentrations of uric acid, and SERS spectra were obtained. Weighted least squares (WLS)[45] was employed in data preprocessing for baseline correction, and MCR-ALS decomposed the matrix (**D**) into its pure response profiles using an initial estimate and assuming that the experimental data followed a linear behavior. Singular value decomposition (SVD) was used to identify the number of significant contributions to the data variance. In this case, two significant contributions (from uric acid and interferences) were identified. To overcome the possibility of rotational ambiguity in the MCR-ALS analysis, a non-negativity constraint for concentrations was employed. The fast non-negative least squares (FNNLS) algorithm was selected as an interactive method with a convergence value of 0.1%.

MCR-ALS recovered the individual SERS spectra (matrix $\mathbf{S}^T$) from the mixed SERS spectra of uric acid and interferences, thereby enabling the analysis of this complex matrix without the necessity to identify and include the interferences in the model (second order advantage).

The recovered SERS spectrum of uric acid was compared with that obtained in aqueous solution (Fig. 5), showing good similarity (correlation of 93%) and confirming that a chemical interpretation of uric acid spectra can be performed even with overlapping bands due to chemical interferences.

MCR-ALS was also used to build a pseudo-univariate curve (Fig. 6A) using recovery values from the **C** matrix relative to uric acid additions. A wide range of uric acid concentrations was added to the synthetic urine (0–25 mmol L^{-1}) to obtain a

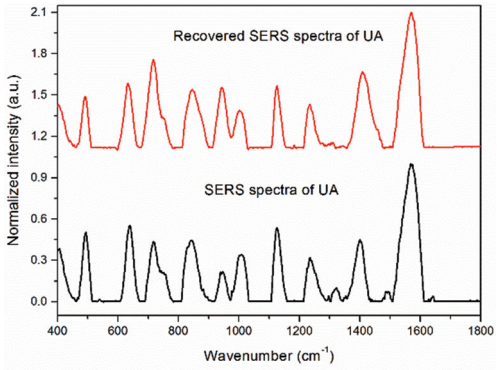

Fig. 5 Comparison between MCR-ALS recovered and expected SERS spectra of uric acid (UA).

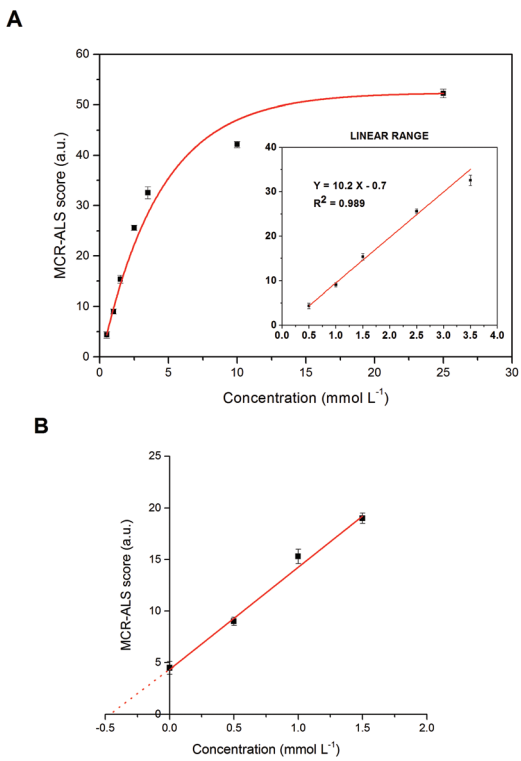

Fig. 6 Linear range for uric acid determinations in synthetic urine (A) and the standard addition curve for the determination of uric acid 0.5 mmol L^{-1} (B).

linear working range for quantifying uric acid. A correlation coefficient (R^2) of 0.989 was found in the range of 0 to 3.5 mmol L^{-1}; linearity was assessed in an analysis of variance (ANOVA) and indicated no significant linearity deviation ($P < 0.05$). Additionally, the standard addition curve used to determine uric acid (0.5 mmol L^{-1}) in synthetic urine is presented in Fig. 6B.

4.4 Analytical method performance

The applicability of the proposed method was validated by assessing the accuracy and precision at three uric acid addition levels (Table 1). There were no significant differences between the expected and calculated concentrations using the proposed method in all the studied levels (Student's *t*-test at a 95% confidence level). The relative error (E_r) was in the range of 3–9%, thereby providing adequate accuracy for uric acid determination (less than 17%) according to the recommendations of the Clinical Laboratory Improvement Amendments (CLIA).[46] Precision, expressed as the relative standard deviation (RSD), varied between 8.7% and 14.8%. These values include the possible variations in inter and across substrates (substrate homogeneity) as well as from batch to batch. Moreover, the limit of detection (LOD) and quantification (LOQ) were 0.11 and 0.36 mmol L^{-1},[47] respectively, thereby demonstrating uric acid determinations at clinically relevant concentrations (≥0.4 mmol L^{-1}) because uric acid levels above 0.4 mmol L^{-1} in the urine and serum can be associated with severe hypertension and proteinuria, which could lead to a diagnosis of preeclampsia.[5,48]

Table 1 Addition and recovery experiment to evaluate accuracy and precision of the proposed method

		Accuracy		Precision
Reference value	Found ± *s* (mmol L^{-1})	Recovery (%)	E_r (%)	RSD (%)
Level 1 (0.5 mmol L^{-1})	0.47 ± 0.07	94	−6	14.8
Level 2 (1 mmol L^{-1})	1.03 ± 0.10	103	+3	9.7
Level 3 (2 mmol L^{-1})	2.18 ± 0.19	109	+9	8.7

A univariate analysis was performed at 493 cm^{-1} (the least overlapped band); notably, similar results to those reported for the electrochemical SERS detection of uric acid were found.[48] However, a reduced correlation coefficient (R^2, 0.960) and reduced precision (RSD, 11–20%) and accuracy (E_r, 13–16%) were noted compared with the MCR-ALS approach. This is in agreement with previous studies, thereby demonstrating the advantages of multivariate over conventional univariate methods in quantitative SERS analysis.[44,49] Thus, in addition to the potential for a chemical interpretation of pure SERS spectra, an MCR-ALS-based method can provide better performance than a conventional univariate method for uric acid determination in synthetic urine and may be easily extended for the determination of other biomarkers even in the presence of interferences. Furthermore, this opens the possibility of using the proposed method for rapid and on-site monitoring of uric acid in the urine of pregnant women, which may lead to early preeclampsia diagnosis.

5. Conclusions

In summary, GNP-coated paper substrates prepared in the proposed procedure result in cost-effective SERS substrates that can be applied for the on-site determination of uric acid with minimum sample preparation. Considerations about the matrix effect demonstrated that an external calibration is not

adequate for quantitative analysis in synthetic urine and that the standard addition method should be used to overcome this problem. The MCR-ALS approach was used to solve the overlapping bands of uric acid and interference SERS spectra as well as presenting adequate performance (accuracy, precision and detection limit) for controlling uric acid. This is the first time that a method based on SERS-coupled chemometrics was employed for the remote determination of uric acid at clinically relevant concentrations. This method could be implemented for the rapid preliminary testing of preeclampsia and the determination of other biomarkers in complex sample matrices.

Acknowledgements

The authors gratefully acknowledge the Conselho Nacional de Desenvolvimento Científico e Tecnológico (CNPq), São Paulo, and Metrohm for providing the portable Raman spectrometer.

References

1 D. M. Carty, C. Delles and A. F. Dominiczak, *Trends Cardiovasc. Med.*, 2008, **18**, 186–194.
2 D. H. Kang, T. Nakagawa, L. Feng, S. Watanabe, L. Han, M. Mazzali, L. Truong, R. Harris and R. J. Johnson, *J. Am. Soc. Nephrol.*, 2002, **13**, 2888–2897.
3 L. Duley, *Semin. Perinatol.*, 2009, **33**, 130–137.
4 L. K. Wagner, *Am. Fam. Physician*, 2004, **70**, 2317–2324.
5 C. S. Buhimschi, E. R. Norwitz, E. Funai, S. Richman, S. Guller, C. J. Lockwood and I. A. Buhimschi, *Am. J. Obstet. Gynecol.*, 2005, **192**, 734–741.
6 E. Akyilmaz, M. K. Sezgintürk and E. Dinçkaya, *Talanta*, 2003, **61**, 73–79.
7 S. M. U. Ali, Z. H. Ibupoto, M. Kashif, U. Hashim and M. Willander, *Sensors*, 2012, **12**, 2787–2797.
8 N. Puri, V. Sharma, V. K. Tanwar, N. Singh, A. M. Biradar and Rajesh, *Prog. Biomater.*, 2013, **2**, 5.
9 E. Dinçkaya, E. Akyilmaz and S. Akgöl, *Indian J. Biochem. Biophys.*, 2000, **37**, 67–70.
10 Y. Yue-dong, *Biomed. Chromatogr.*, 1998, **12**, 47–49.
11 S. L. Yan, P. Z. Lin and M. W. Hsiao, *J. Chromatogr. Sci.*, 1999, **37**, 45–50.
12 P. R. Carey, *J. Biol. Chem.*, 1999, **274**, 26625–26628.
13 M. Pérez-Alonso, K. Castro and J. M. Madariaga, *Anal. Chim. Acta*, 2006, **571**, 121–128.
14 P. Vítek, E. M. a. Ali, H. G. M. Edwards, J. Jehlička, R. Cox and K. Page, *Spectrochim. Acta, Part A*, 2012, **86**, 320–327.
15 J. Jehlička, P. Vítek, H. G. M. Edwards, M. Heagraves and T. Čapoun, *Spectrochim. Acta, Part A*, 2009, **73**, 410–419.
16 B. S. Luo and M. Lin, *J. Rapid Methods Autom. Microbiol.*, 2008, **16**, 238–255.
17 G. McNay, D. Eustace, W. E. Smith, K. Faulds and D. Graham, *Appl. Spectrosc.*, 2011, **65**, 825–837.
18 P. G. Etchegoin and E. C. Le Ru, in *Surface enhanced Raman spectroscopy: analytical, biophysical and life science applications*, ed. S. Schlücker, Wiley-VCH, Weinheim, Germany, 2010, ch. 1, pp. 1–37.
19 M. Fan, G. F. S. Andrade and A. G. Brolo, *Anal. Chim. Acta*, 2011, **693**, 7–25.
20 P. Ndokoye, J. Ke, J. Liu, Q. Zhao and X. Li, *Langmuir*, 2014, **30**, 13491–13497.
21 S. Benítez-Martínez, A. I. López-lorente and M. Valcárcel, *Microchem. J.*, 2015, **121**, 6–13.
22 A. K. M. Jamil, E. L. Izake, A. Sivanesan and P. M. Fredericks, *Talanta*, 2015, **134**, 732–738.
23 N. P. W. Pieczonka and R. F. Aroca, *Chem. Soc. Rev.*, 2008, **37**(5), 946–954.
24 C. De Bleye, E. Dumont, E. Rozet, P.-Y. Sacré, P.-F. Chavez, L. Netchacovitch, G. Piel, P. Hubert and E. Ziemons, *Talanta*, 2013, **116**, 899–905.
25 M. B. Mamián-López and R. J. Poppi, *Anal. Chim. Acta*, 2013, **760**, 53–59.
26 S. Ito and K. Tsukada, *J. Chromatogr., A*, 2002, **943**, 39–46.
27 E. Comas, R. a. Gimeno, J. Ferre, R. M. Marce, F. Borrull and F. X. Rius, *J. Chromatogr., A*, 2004, **1035**, 195–202.
28 E. Peré-Trepat, S. Lacorte and R. Tauler, *J. Chromatogr., A*, 2005, **1096**, 111–122.
29 A. de Juan, J. Jaumot and R. Tauler, *Anal. Methods*, 2014, **6**, 4964–4976.
30 R. Tauler, *Chemom. Intell. Lab. Syst.*, 1995, **30**, 133–146.
31 W. Windig and J. Guilment, *Anal. Chem.*, 1991, **63**, 1425–1432.
32 C. D. L. Albuquerque and R. J. Poppi, *Anal. Chim. Acta*, 2015, **879**, 24–33.
33 J. Jaumot, A. de Juan and R. Tauler, *Chemom. Intell. Lab. Syst.*, 2015, **140**, 1–12.
34 J. Turkevich, P. C. Stevenson and J. Hillier, *Discuss. Faraday Soc.*, 1951, **11**, 55–75.
35 B. R. Shmaefsky, *Am. Biol. Teach.*, 1990, **52**, 170–172.
36 T. Brooks and C. W. Keevil, *Lett. Appl. Microbiol.*, 1997, **24**, 203–206.
37 P. N. Njoki, I. I. S. Lim, D. Mott, H. Y. Park, B. Khan, S. Mishra, R. Sujakumar, J. Luo and C. J. Zhong, *J. Phys. Chem. C*, 2007, **111**, 14664–14669.
38 S. Hong and X. Li, *J. Nanomater.*, 2013, **2013**, 790323.
39 S. E. J. Bell and M. R. McCourt, *Phys. Chem. Chem. Phys.*, 2009, **11**, 7455–7462.
40 Y. H. Ngo, D. Li, G. P. Simon and G. Garnier, *Langmuir*, 2012, **28**, 8782–8790.
41 Y. H. Ngo, D. Li, G. P. Simon and G. Garnier, *J. Colloid Interface Sci.*, 2013, **392**, 237–246.
42 L. Polavarapu and L. M. Liz-Marzán, *Phys. Chem. Chem. Phys.*, 2013, **15**, 5288–5300.
43 A. Shiohara, Y. Wang and L. M. Liz-Marzán, *J. Photochem. Photobiol., C*, 2014, **21**, 2–25.
44 Y. Fan, K. Lai, B. A. Rasco and Y. Huang, *Food Control*, 2014, **37**, 153–157.

45 Z. M. Zhang, S. Chen and Y. Z. Liang, *Analyst*, 2010, **135**, 1138–1146.
46 US Department of Health and Human Services, Regulations Implementing the Clinical Laboratory Improvement Amendments of 1988 (CLIA). Final rule. Federal Register, 1992, **57**, 7002–7186.
47 J. Saurina, C. Leal, R. Compañó, M. Granados, M. D. Prat and R. Tauler, *Anal. Chim. Acta*, 2001, **432**, 241–251.
48 L. Zhao, J. Blackburn and C. L. Brosseau, *Anal. Chem.*, 2015, **87**, 441–447.
49 Y. Fan, K. Lai, B. A. Rasco and Y. Huang, *LWT—Food Sci. Technol.*, 2015, **60**, 352–357.